Fraunhofer Institut
Techno- und
Wirtschaftsmathematik

M. Krekel

Optimal portfolios with a loan dependent credit spread

Berichte des Fraunhofer ITWM, Nr. 32 (2002)

ISSN 1434-9973

Bericht 32 (2002)

Die Veröffentlichungen in der Berichtsreihe des Fraunhofer ITWM können bezogen werden über:

Fraunhofer-Institut für Techno- und
Wirtschaftsmathematik ITWM
Gottlieb-Daimler-Straße, Geb. 49

67663 Kaiserslautern

Telefon: +49 (0) 6 31/2 05-32 42
Telefax: +49 (0) 6 31/2 05-41 39
E-Mail: info@itwm.fhg.de
Internet: www.itwm.fhg.de

Vorwort

Das Tätigkeitsfeld des Fraunhofer Instituts für Techno- und Wirtschaftsmathematik ITWM umfasst anwendungsnahe Grundlagenforschung, angewandte Forschung sowie Beratung und kundenspezifische Lösungen auf allen Gebieten, die für Techno- und Wirtschaftsmathematik bedeutsam sind.

In der Reihe »Berichte des Fraunhofer ITWM« soll die Arbeit des Instituts kontinuierlich einer interessierten Öffentlichkeit in Industrie, Wirtschaft und Wissenschaft vorgestellt werden. Durch die enge Verzahnung mit dem Fachbereich Mathematik der Universität Kaiserslautern sowie durch zahlreiche Kooperationen mit internationalen Institutionen und Hochschulen in den Bereichen Ausbildung und Forschung ist ein großes Potenzial für Forschungsberichte vorhanden. In die Berichtreihe sollen sowohl hervorragende Diplom- und Projektarbeiten und Dissertationen als auch Forschungsberichte der Institutsmitarbeiter und Institutsgäste zu aktuellen Fragen der Techno- und Wirtschaftsmathematik aufgenommen werden.

Darüberhinaus bietet die Reihe ein Forum für die Berichterstattung über die zahlreichen Kooperationsprojekte des Instituts mit Partnern aus Industrie und Wirtschaft.

Berichterstattung heißt hier Dokumentation darüber, wie aktuelle Ergebnisse aus mathematischer Forschungs- und Entwicklungsarbeit in industrielle Anwendungen und Softwareprodukte transferiert werden, und wie umgekehrt Probleme der Praxis neue interessante mathematische Fragestellungen generieren.

Prof. Dr. Dieter Prätzel-Wolters
Institutsleiter

Kaiserslautern, im Juni 2001

Optimal portfolios with a loan dependent credit spread

This version
January 18, 2002

Martin Krekel
Fraunhofer ITWM, Department of Financial Mathematics, 67653 Kaiserslautern, Germany

Abstract: If an investor borrows money he generally has to pay higher interest rates than he would have received, if he had put his funds on a savings account. The classical model of continuous time portfolio optimisation ignores this effect. Since there is obviously a connection between the default probability and the total percentage of wealth, which the investor is in debt, we study portfolio optimisation with a control dependent interest rate. Assuming a logarithmic and a power utility function, respectively, we prove explicit formulae of the optimal control.

Keywords and phrases: Portfolio optimisation, stochastic control, HJB equation, credit spread, log utility, power utility, non-linear wealth dynamics.

1 Introduction

The continuous-time portfolio problem was first introduced by Merton in his pioneering works from 1969 and 1971. His goal is to find a suitable investment strategy which maximises the expected utility of the final wealth. In the case of logarithmic and power utility this yields the result that it is optimal to invest a constant multiple of the total wealth in stocks. With common market parameters this factor is mostly bigger than one. In other words, the investor is advised to borrow a multiple of his own wealth to speculate in risky assets. Of course in the presence of possible crashes no rational investor would do so, because this can result in immediate bankruptcy . On the other hand, since the default probability of this particular credit is much higher, the counterpart who is lending the money will definitly claim higher yields than that for government bonds. In addition, in a single stock setting, this yield should converge (w.r.t. control) to the return of the stock, since the risk of the lender will be almost the same, as if he invests in the stock itself. We introduce a control dependent interest rate, i.e. credit spread, to take this credit risk into account.

2 Model

We consider a security market consisting of an interest-bearing cash account and n risky assets. The uncertainty is modelled by a probability space $(\Omega, \mathcal{F}, \{\mathcal{F}\}_{t\in[0,T]}, P)$. The flow of information is given by the natural filtration $\mathcal{F}_t$, i.e. the P-augmention of an n-dimensional Brownian filtration. Without loss of generality we set $\mathcal{F}_T = \mathcal{F}$, so that all observable events are eventually known. In addition we make the assumptions that the market is frictionless except for the non-constant interest rate. All traders are assumed to be price takers, and there are no transaction costs. The cash account is modelled by the differential equation

$$dB(t) = B(t)R(t)dt,$$

where $R(t)$ is a bounded, strictly positive and progressively measurable process. We will in particular assume different interest rates for borrowing and lending. This feature will be modelled via a control dependent interest rate $R(t) = r(\pi_t)$, where $r(.) : \mathbb{R}^n \to \mathbb{R}$ is a left continuous and bounded function, which will be defined later on. The price process of the i-th, $i = 1, \ldots, n$, risky asset is given by

$$dP_i(t) = P_i(t)[b_i dt + \sum_{j=1}^{n} \sigma_{ij} dW_j(t)],$$

with $\sigma\sigma'$ a strictly positive definite $N \times N$-matrix. The investor starts with an initial wealth $x_0 > 0$ at time $t = 0$. In the beginning this initial wealth is invested in different assets and he is allowed to adjust his holdings continuously up to a fixed planning horizon T. His investment behavior is modelled by a portfolio process $\pi(t) = (\pi_1(t), \ldots, \pi_n(t))$ which is progressively measurable and denotes the percentage of total wealth invested in the particular stocks. If $\sum_{i=1}^n \pi_i \leq 1$, $1 - \sum_{i=1}^n \pi_i$ is the percentage invested in a savings account. If $\sum_{i=1}^n \pi_i > 1$ the investor is actually borrowing money and the credit spread comes into the game. We are considering self-financing portfolio processes, thus the wealth process follows the stochastic differential equation

$$dX(t) = X(t)\big[\,\big(\,r(\pi(t))(1 - \pi'(t)\underline{1}) + \pi'(t)b\,\big)dt + \pi'(t)\sigma dW(t)\,\big], \tag{1}$$

with $X(0) = x_0$. Note that the presence of $r(\pi(t))$ introduces a non-linear dependence of the wealth process from $\pi(t)$. The investor is only allowed to choose a portfolio process which is admissible and thus leads to a positive wealth process X^π. The final wealth is given by:

$$X^\pi(T) = x_0 e^{\int_0^T \left(r(\pi(t))(1-\pi'(t)\underline{1})+\pi'(t)b-\frac{1}{2}\pi'(t)\sigma\sigma'\pi(t) \right)dt+\int_0^T \pi'(t)\sigma dW(t)} \tag{2}$$

We want to solve the following optimisation problem

$$\max_{\pi(.)\in\mathcal{A}(0,x_0)} E(U(X^\pi(T))), \tag{3}$$

where U is the utility function of the investor. The set $\mathcal{A}(0, x_0)$ contains the admissible controls with initial condition $(0, x_0)$, "sufficiently" bounded and a corresponding wealth process X^π greater or equal to zero for all t in $[0, T]$ almost surely. See Korn/Korn (2001) for an exact definition. Note that the properties of $r(.)$ ensure the existence of a solution of the SDE (1). The term (3) raises the question, if the maximum exists. Or in other words: Is there a control $\pi^*(.) \in \mathcal{A}(0, x_0)$, such that $E(U(X^{\pi^*}(T))) = \sup_{\pi(.)\in\mathcal{A}(0,x_0)} E(U(X^\pi(T)))$? Via a verification theorem we will show that this is actually true.

We suggest three ways of modelling $r(.)$ which should cover all practical needs, and also prove to be quite usefull for numerical calculations. Let $\bar{r}$ be the interest rate for a positive cash account and $u'\underline{1} = \sum_{i=1}^n u_i$ the total percentage of wealth invested in stocks:

1. Step function

$$r(u) = \bar{r} \ + \sum_{i=0}^{m-1} \lambda_i \mathbf{1}_{(\alpha_i,\alpha_{i+1}]}(u'\underline{1}) \tag{4}$$

   where $-\infty = \alpha_0 < 1 \leq \alpha_1 < \ldots < \alpha_i < \alpha_{i+1} < \ldots < \alpha_m = \infty$ and
   $0 = \lambda_0 < \lambda_1 < \ldots < \lambda_i < \lambda_{i+1} < \ldots < \lambda_{m-1} < \infty$.

2. Frequency polygon

$$\begin{aligned} r(u) &= \bar{r} \ + \sum_{i=0}^{m-1} (r_i + \mu_i(u-\alpha_i))\mathbf{1}_{[\alpha_i,\alpha_{i+1})}(u'\underline{1}) \\ r_i &= \sum_{j=1}^{i} \mu_{j-1}(\alpha_j - \alpha_{j-1}) \quad i \geq 1 \end{aligned} \tag{5}$$

   where $-\infty = \alpha_0 < 1 \leq \alpha_1 < \ldots < \alpha_i < \alpha_{i+1} < \ldots < \alpha_m = \infty$,
   $\mu_i \geq 0$ for all $i = 1, \ldots, m-2$ and $\mu_0 = 0 = \mu_{m-1}, r_0 = 0$.

3. Logistic function

$$r(u) = \bar{r} \ + \lambda \frac{e^{\alpha u'\underline{1}+\beta}}{e^{\alpha u'\underline{1}+\beta}+1} \tag{6}$$

   with $\lambda > 0$,$\alpha > 0$.

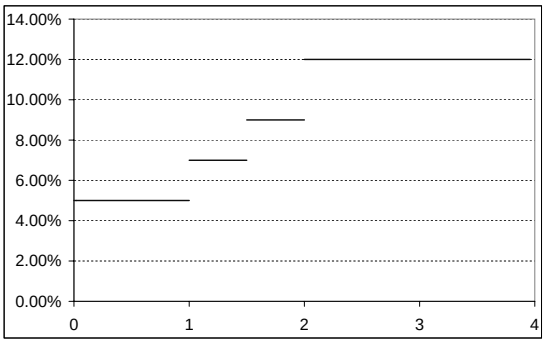

Figure 1: Step function

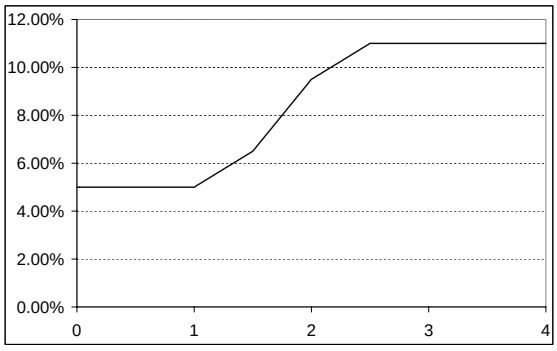

Figure 2: Frequency polygon

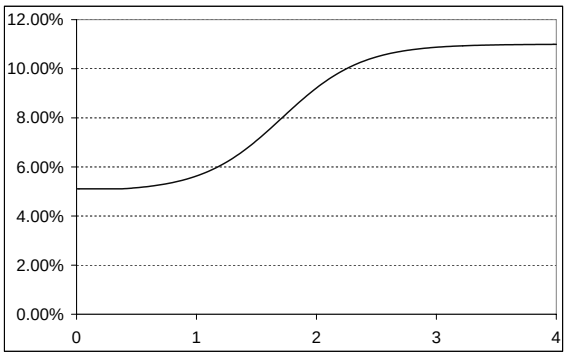

Figure 3: Logistic function

Simple dependencies, like $r(u) = \bar{r}$ for $u'\underline{1} \leq 1$ and $r(u) = \bar{r} + \lambda$ for $u'\underline{1} > 1$ can be modelled with the help of the step function. See Korn (1995) for the treatment of an option pricing problem in the presence of such a setting. With the frequency polygon we are able to model smoothly increasing credit spreads. In the these cases, the optimisation problem (3) can be solved analytically, although we have to deal with some subcases separately.
The logistic function can be unterstood as a continuous approximation of a frequency polygon with just one triangle. The main reason for its introduction is for numerical computations, because it is twice contiuously differentiable and can be handled without considering subcases separately. An analytical solution is not available, but this does not matter with regard to the use in numerical context.

In section 3 we solve the optimisation problem for logarithmic utility ($U(x) = \ln(x)$) and in section 4 for power utility, that means $U(x) = \frac{1}{\gamma}x^{\gamma}$ with $\gamma \in (-\infty, 0) \cup (0, 1)$. Section 5 gives a conclusion.

3 Logarithmic Utility

Let $U(x) = \ln(x)$, then we have the following optimisation problem

$$V(t,x) := \sup_{\pi(.)\in\mathcal{A}(t,x)} E^{t,x}(\ln(X^{\pi}(T))) \tag{7}$$

$$= \sup_{\pi(.)\in\mathcal{A}(t,x)} \left\{ \ln(x) + E\left[\int_t^T \big(r(\pi(t))(1-\pi'(t)\underline{1}) + \pi'(t)b - \frac{1}{2}\pi'(t)\sigma\sigma'\pi(t)\big)dt\right] + E\left[\int_t^T \pi'(t)\sigma dW(t)\right]\right\},$$

where r is given by (4),(5) or (6). Using Fubini's Theorem for $\pi(t) \in L^2[0,T]$ then yields:

$$V(t,x) = \ln(x) + \sup_{\pi(.)\in\mathcal{A}(t,x)} \int_t^T E\left[\big(r(\pi(t))(1-\pi'(t)\underline{1}) + \pi'(t)b - \frac{1}{2}\pi'(t)\sigma\sigma'\pi(t)\big)\right] dt$$

$$\leq \ln(x) + \int_t^T \sup_{\{\hat{\pi}(t):\mathcal{F}_t-\text{meas.}\}} E\left[\big(r(\hat{\pi}(t))(1-\hat{\pi}'(t)\underline{1}) + \hat{\pi}'(t)b - \frac{1}{2}\pi'(t)\sigma\sigma'\pi(t),\big)\right] dt$$

Notice, that we changed from functional to pointwise optimisation, which leads to the inequality sign. Since there is nothing stochastic or time-dependent within the brackets of the expected value (besides the control process $\hat{\pi}(t)$ which however is at our disposal), we obtain:

$$V(t,x) \leq \ln(x) + \sup_{u\in\mathbb{R}^n} \big\{ r(u)(1-u'\underline{1}) + u'b - \frac{1}{2}u'\sigma\sigma'u\big\}(T-t) \tag{8}$$

We need the following notations to study the question of the existence of a maximum:

$$D_i := \{(x_1,\ldots,x_n)' : \alpha_i < \sum_{i=1}^n x_i \leq \alpha_{i+1}\} \tag{9}$$

$$H_i := \{x \in \mathbb{R}^n : \sum_{i=1}^n x_i = \alpha_i\} \tag{10}$$

$$\overline{D_i} := D_i \cup H_i \tag{11}$$

$$M_i^{S\theta}(x) := (\bar{r} + \lambda_i)(1-x'\underline{1}) + x'b - \frac{1}{2}\Theta x'\sigma\sigma'x \tag{12}$$

where $i = 0,\ldots,m-1$. Observe that $\{D_i\}_{i=0,\ldots,m-1}$ is a partition of $\mathbb{R}^n$, i.e. $\mathbb{R}^n = \bigcup_{i=0}^{m-1} D_i$, and $\overline{D_i} \cap U = (H_i \cup D_i) \cap U$ for any compact $U \subset \mathbb{R}^n$.

Proposition 1 : Existence of the maximum
Let:

$$M^{\theta}(x) := r(x)(1-x'\underline{1}) + x'b - \frac{1}{2}\Theta x'\sigma\sigma'x \tag{13}$$

with r(x) being either a step function, frequency polygon or logistic function as given (4-6) and $\Theta \in (0,\infty)$. Then there is an $x^* \in U = \bar{D}_c(\underline{0}) = \{x \in \mathbb{R}^n : \|x - (0,\ldots,0)\| \leq c\}$, for a suitable c, such that we have:

$$\sup_{x\in\mathbb{R}^n} M^{\theta}(x) = M^{\theta}(x^*) \quad \text{or} \quad x^* = \arg\max_{x\in U} M^{\theta}(x)$$

PROOF:
Boundness: Recall that $\sigma\sigma'$ is strictly positive definite and and $r(x)$ is bounded. Thus, $M^\theta(x)$ is bounded from above and $M^\theta(x) \to -\infty$ if $\|x\| \to \infty$. Hence, $\sup_{x\in\mathbb{R}^n} M^\theta(x) = \sup_{x\in U} M^\theta(x)$ and $\sup_{x\in D_i} M^\theta(x) = \sup_{x\in D_i\cap U} M^\theta(x)$ $(i = 0,\ldots,m-1)$ for U sufficiently large and compact.

Existence: If $r(x)$ is a *frequency polygon* or a *logistic function*, the existence of the maximum follows by continuity of M^θ and compactness of U.

Let $r(x)$ be a *step function* as given in (4). Observe, that for all $x \in H_{i+1}$, $i = 0,\ldots,m-2$, we have $M_i^{S\theta}(x) \geq M_{i+1}^{S\theta}(x)$, since $\lambda_i < \lambda_{i+1}$ and $x'\underline{1} \geq 1$ in H_{i+1}. Because $M_i^{S\theta}$ is continuous we get:

$$\sup_{x\in U} M^\theta(x) \quad = \quad \max_i \sup_{x\in D_i\cap U} M_i^{S\theta}(x) = \max_i \max_{x\in\overline{D_i\cap U}} M_i^{S\theta}(x)$$

Hence there exists a j and $x_j \in D_j$, such that $\sup_{x\in U} M^\theta(x) = M_j^{S\theta}(x_j)$. If $x_j \in H_j$, then $M_{j-1}^{S\theta}(x_j) > M_j^\theta(x_j)$, which is a contradiction. Thus $x_j \in D_j$ and $\sup_{x\in U} M^\theta(x) = M^\theta(x_j)$. Consequently,

$$x^* = \arg\max_{x\in U} M^\theta(x) \Rightarrow \sup_{x\in U} M^\theta(x) = M^\theta(x^*).$$

□

Define:

$$\pi^*(.) \quad \equiv u^* = \quad \arg\max_x \left\{ r(u)(1 - x'\underline{1}) + x'b - \frac{1}{2}x'\sigma\sigma'x \right\} \tag{14}$$

Since $\pi^*(.)$ is constant, it is an element of $\mathcal{A}(0,x_0)$, thus the original problem (7) has been solved too. We summarize this in

Theorem 1 : Verification with logarithmic utility
The constant process π^* defined by $\pi^*(t) = u^* \forall t \in [0,T]$ as given in (14) is the optimal control and

$$V(t,x) = \ln(x) + \left(r(u^*)(1 - u^{*\prime}\underline{1}) + u^{*\prime}b - \frac{1}{2}u^{*\prime}\sigma\sigma'u^* \right)(T-t).$$

PROOF: From Proposition 1 and (8) we obtain:

$$E^{t,x}(\ln(X^{\pi^*}(T))) \leq V(t,x) \leq \underbrace{\ln(x) + \left(r(u^*)(1 - u^{*\prime}\underline{1}) + u^{*\prime}b - \frac{1}{2}u^{*\prime}\sigma\sigma'u^* \right)(T-t)}_{=E^{t,x}(\ln(X^{\pi^*}(T)))}$$

□

The remaining questions is, how to determine the optimal control. If $r(u)$ is a step function or a frequency polygon as given in (4,5), we can determine the maximum explicitly, by using $\{D_i\}_{i=0,\ldots,m-1}$ the partition of $\mathbb{R}^n$. We investigate $M_i^\theta(x)$ separately on the sets $\overline{D_i}$. Since $M_i^\theta(x)$ are downwards opened parabolas (in both cases), we can determine the local maxima. Then we compare these maxima to obtain the absolute maximum and the corresponding optimal control.
If $r(u)$ is a logistic function, we have to calculate the maximum via numerical methods. We consider all these cases explicitly below:

3.1 Step function

Theorem 2 : Optimal Portfolios with step functions and power utility

Let $V^S(t,x)$ be the value function given in (7) with $r(u)$ a step function defined by (4). In addition, let $M^{S\Theta}$ be the function to be maximised in Proposition 1 corresponding to the step function $r(u)$, i.e.

$$M^{S\Theta}(u) = \left[\bar{r} + \sum_{i=0}^{m-1} \lambda_i \mathbf{1}_{(\alpha_i,\alpha_{i+1}]}(u'\underline{1})\right](1-u'\underline{1}) + u'b - \frac{1}{2}\Theta u'\sigma\sigma' u, \qquad (15)$$

where λ_i and α_i are given in (4). Then there exists an optimal (constant) control $\pi^*(.) = u^* = \arg\max_{u\in\mathbb{R}^n} M^{S1}(u)$ such that

$$V^S(t,x) \equiv \sup_{\pi(.)\in\mathcal{A}(t,x)} E^{t,x}(\ln(X^\pi(T))) = E^{t,x}(\ln(X^{\pi^*}(T))) \quad .$$

The value u^* is explicitly given below (with $\Theta = 1$):

1. *One-dimensional case*

$$u^* = \arg \max_{\{u_i : i=0,\ldots,m-1\}} \left\{M_i^{S\theta}(u_i)\right\}$$

$$u_i = \max\left(\alpha_i, \min\left(\alpha_{i+1}, \frac{b-r-\lambda_i}{\Theta\sigma^2}\right)\right)$$

2. *Multidimensional case*

$$u^* = \arg \max_{\{u_i : i=0,\ldots,m-1\}} \left\{M_i^{S\theta}(u_i)\right\}$$

whereby

$$u_i = \begin{cases} \frac{1}{\theta}(\sigma^*\sigma^{*\prime})^{-1}b^{*u} & : \ v_i \notin \overline{D_i} \ \wedge \ \text{dist}(H_i, v_i) > \text{dist}(H_{i+1}, v_i) \\ v_i & : \ v_i \in \overline{D_i} \\ \frac{1}{\theta}(\sigma^*\sigma^{*\prime})^{-1}b^{*d} & : \ v_i \notin \overline{D_i} \ \wedge \ \text{dist}(H_i, v_i) < \text{dist}(H_{i+1}, v_i) \end{cases}$$

with

$$v_i = \frac{1}{\theta}(\sigma\sigma')^{-1}\left(b - (\bar{r} + \lambda_i)\underline{1}\right)$$

and $\sigma^* \in \mathbb{R}^{(n-1)\times(n-1)}$ with $\sigma^*_{ki} = \sigma_{ki} - \sigma_{ni}$ and $b^{*u}_k = b_k - b_n - \theta\alpha_{i+1}\sum_{i=1}^n \sigma_{ni}\sigma^*_{ki}$ resp. $b^{*d}_k = b_k - b_n - \theta\alpha_i \sum_{i=1}^n \sigma_{ni}\sigma^*_{ki}$.

Proof: As proved in Theorem 1, the optimal control exists and is given by:

$$\pi^*(.) \equiv u^* = \arg \max_{x\in\mathbb{R}^n} M^{S\Theta}(x)$$

with $\Theta = 1$. We include a real number $\Theta \in (0,\infty)$ in front of the quadratic term, because we will use this Theorem in the next chapter. As stated in the proof of Proposition 1:

$$\max_{x\in\mathbb{R}^n} M^{S\theta}(x) = \max_i \max_{x\in\overline{D_i}} M_i^{S\theta}(x)$$

So:

$$\arg\max_{u\in U} M^{\theta}(x) \quad = \quad \arg\max_{u_i} M_i^{S\theta}(u_i) \text{ with } u_i = \arg\max_{u\in\overline{D_i}} M_i^{S\theta}(u)$$

As before mentioned, we achieve the local maxima and corresponding arguments on the sets $\overline{D_i}$ and then we compare them to obtain the absolute maximum. Thus only the verification of u_i is left.

One-dimensional case
The $M_i^{S\theta}(x)$ are downwards opening parabolas; so we just have to determine the apex (ignoring the domain $\overline{D_i}$) and check its position relative to $\overline{D_i}$. If the apex is in $\overline{D_i} = [\alpha_i, \alpha_{i+1}]$ we have already found the maximum. If it lies on the right(left) side of the intervall, the maximum is achieved in α_{i+1} (α_i) .

Multidimensional case
Again, the first step is to determine the apex without any restrictions on the domain.

$$\begin{aligned} v_i \quad &:= \quad \arg\max_{u\in\mathbb{R}^n} \left\{(\bar{r} \ +\lambda_i)(1-u'\underline{1}) + u'b - \frac{1}{2}\Theta u'\sigma\sigma' u\right\} \qquad (16)\\ &= \quad \frac{1}{\Theta}(\sigma\sigma')^{-1}\left(b-(\bar{r} \ +\lambda_i)\underline{1}\right) \end{aligned}$$

Observe, that $\sigma\sigma'$ is regular, as stated in Proposition 1. If $v_i \in \overline{D_i}$, then we have found the local maximum and so we can say $u_i = v_i$.
If $v_i \notin \overline{D_i}$, then the local maximum must lie in one of the hyperplanes H_i respectively H_{i+1}, since $-\sigma\sigma'$ is strictly negative definite and $M_i^{S\Theta}$ therefore strictly concave. If $\text{dist}(H_i, v_i) > (<) \text{ dist}(H_{i+1}, v_i)$ then u_i lies in H_{i+1} (H_i). Thus we have to calculate the maximum under the constraint $u'\underline{1} = \alpha$, with $\alpha = \alpha_i$ resp. $\alpha = \alpha_{i+1}$, thus $u_n = \alpha - \sum_{k=1}^{n-1} u_k$.
In the following we have to use the components of the vector u and b explicitly to do our calculations. Thus we will neglect the index i of λ_i and v_i to avoid confusion:

$$\begin{aligned} v \quad &= \quad \arg\max_{u\in H}\left\{(\bar{r} \ +\lambda)(1-u'\underline{1}) + u'b - \frac{1}{2}\Theta u'\sigma\sigma' u\right\}\\ &= \quad \arg\max_{u\in\mathbb{R}^{n-1}}\left\{\bar{r} \ +\lambda + \sum_{k=1}^{n-1} u_k(b_k - \bar{r} \ -\lambda) + (\alpha - \sum_{k=1}^{n-1} u_k)(b_n - \bar{r} \ -\lambda)\right.\\ &\qquad\qquad \left. -\frac{1}{2}\Theta\sum_{i=1}^{n}\left(\sum_{k=1}^{n-1} u_k\sigma_{ki} + (\alpha - \sum_{k=1}^{n-1} u_k)\sigma_{ni}\right)^2\right\}\\ &= \quad \arg\max_{u\in\mathbb{R}^{n-1}}\left\{\bar{r} \ +\lambda + \sum_{k=1}^{n-1} u_k(b_k - b_n) + \alpha(b_n - \bar{r} \ -\lambda)\right.\\ &\qquad\qquad \left. -\frac{1}{2}\Theta\sum_{i=1}^{n}\left(\sum_{k=1}^{n-1} u_k(\sigma_{ki} - \sigma_{ni}) + \alpha\sigma_{ni}\right)^2\right\} \end{aligned}$$

Now let $b^* \in \mathbb{R}^{n-1}$ with $b_k^* = b_k - b_n (k = 1, \ldots, n-1)$ and $\sigma^* \in \mathbb{R}^{(n-1)\times(n-1)}$ with $\sigma_{ki}^* = \sigma_{ki} - \sigma_{ni}$ $(k = 1, \ldots, n-1)$. Observe, that $\text{rank}(\sigma^*) = n-1$, since otherwise we would

get the contradiction $\text{rang}(\sigma) < n$. Thus σ^* is regular. So:

$$\begin{aligned} v &= \arg\max_{u\in\mathbb{R}^{n-1}} \left\{ (1-\alpha)(\bar{r} + \lambda) + \alpha b_n + \sum_{k=0}^{n-1} u_k b_k^* + \right. \\ &\qquad \left. -\frac{1}{2}\Theta \sum_{i=1}^{n} \left(\left(\sum_{k=1}^{n-1} u_k \sigma_{ki}^* \right)^2 + 2\alpha\sigma_{ni} \sum_{k=1}^{n-1} u_k \sigma_{ki}^* + \alpha^2 \sigma_{ni}^2 \right) \right\} \\ &= \arg\max_{u\in\mathbb{R}^{n-1}} \left\{ (1-\alpha)(\bar{r} + \lambda) + \alpha b_n - \frac{1}{2}\Theta \sum_{i=1}^{n} \alpha^2 \sigma_{ni}^2 \right. \\ &\qquad \left. + \sum_{k=1}^{n-1} u_k \left(b_k^* - \Theta\alpha \sum_{i=1}^{n} \sigma_{ni}\sigma_{ki}^* \right) - \frac{1}{2}\Theta \sum_{i=1}^{n} \left(\left(\sum_{k=1}^{n-1} u_k \sigma_{ki}^* \right)^2 \right) \right\} \end{aligned}$$

Thus, with $b_k^{**} = b_k^* - \Theta\alpha \sum_{i=1}^{n} \sigma_{ni}\sigma_{ki}^*$, we obtain the usual representation

$$v = \arg\max_{u\in\mathbb{R}^{n-1}} \left\{ (1-\alpha)(\bar{r} + \lambda) + \alpha b_n - \frac{1}{2}\Theta \sum_{i=1}^{n} \alpha^2 \sigma_{ni}^2 + u' b^{**} - \frac{1}{2}\Theta u' \sigma^* \sigma^{*\prime} u \right\}$$

which yields the solution:

$$v = \frac{1}{\Theta}(\sigma^* \sigma^{*\prime})^{-1} b^{**}$$

□

Remark 1
Note, that v does not depend on λ or $\bar{r}$, because these quantities are fixed on the hyperplanes H_i. If the apex of the i-th parabola is achieved in the sets $\{\overline{D_j} : j \le i\}$, then the absolute maximum can not lie in one of the sets $\{\overline{D_j} : j > i\}$, because $\arg\max_{\{x\in\bigcup_{j\ge i}\overline{D_j}\}} M_i^{S\theta} \in \overline{D_i}$ and $M_i^{S\theta}(x) > M^{S\theta}(x) \forall x \in \bigcup_{j\ge i} \overline{D_j}$ (via $\lambda_i < \lambda_{i+1}$). So, if we are stepwise increasing i (beginning at 0) we can stop the maximum-search, if the above condition is fullfilled. Loosely speaking: The maximum can only be achieved on an apex of $M_i^{S\Theta}$ or downwards-left from it, because λ_i is increasing in i. In the one-dimensional case we see from the above equations that this method can be used to bound $\pi(t)$ by an arbitrary boundary α_m choosing $\lambda_{m-1} = b - r$.

Example 1
Let $r(u)$ be modelled as in Figure 1, i.e.

$$r(u) = \begin{cases} 5\% & : \quad u \le 1 \\ 7\% & : \quad 1 < u \le 1.5 \\ 9\% & : \quad 1.5 < u \le 2 \\ 12\% & : \quad 2.5 < u \end{cases},$$

Let $b = 12\%$ and $\sigma = 20\%$. Then $\pi^*(.) = \frac{12\%-7\%}{20\%^2} = 1.25$. For comparison: If we would have $r(u) \equiv 5\%$ then the optimal control yields $\frac{12\%-5\%}{20\%^2} = 1.75$.

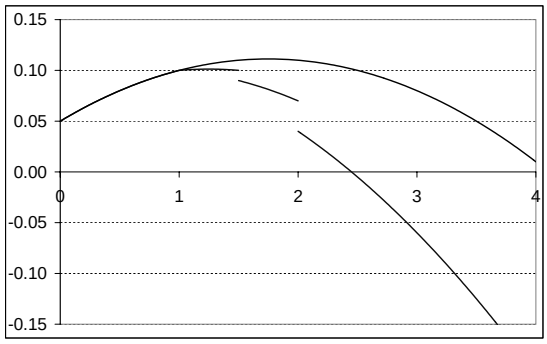

Figure 4: Parabolas M^{S1} with r step function and flat

In Figure 4 we plotted the corresponding function M^{S1} (to be maximised) with r modelled as step function and with r flat. Note, that there are generally jumps at α_i, except for the case when $\alpha_i = 1.0$. Since the coefficient of $r(u)$ is (1-u), the parabola is continuous in 1.0, although $r(u)$ jumps at that point.

3.2 Frequency polygon

The procedure is similar to the one for step functions, i.e. we determine the maxima piecewise on $\overline{D_i}$ and then we compare them to obtain the absolute maximum. In preparation for the next section, we again include a parameter $\theta \in (0, \infty)$ in front of the square term.

Theorem 3 : Optimal Portfolios with polygons and logarithmic utility

Let $V^P(t,x)$ be the value function given in (7) with $r(u)$ frequency polygon defined by (5). In addition, let $M^{P\Theta}$ be the corresponding function to be maximised in Proposition 1 with $r(u)$ frequency polygon, i.e.

$$M^{P\theta}(u) = \left[\bar{r} + \sum_{i=0}^{n-1}(r_i + \mu_i(u'\underline{1} - \alpha_i))\mathbf{1}_{[\alpha_i,\alpha_{i+1})}(u'\underline{1})\right](1 - u'\underline{1}) + u'b - \frac{1}{2}\Theta u'\sigma\sigma' u,$$

with α_i, μ_i, r_i given in (5). Then there exists a constant control $\pi^*(.) = u^* = \arg\max_{u\in\mathbb{R}^n} M^{P\theta}(u)$ such that

$$V^P(t,x) \equiv \sup_{\pi(.)\in\mathcal{A}(t,x)} E^{t,x}(\ln(X^\pi(T))) = E^{t,x}(\ln(X^{\pi^*}(T))) \quad .$$

The value u^* is explicitly given below (with $\Theta = 1$):

1. *One-dimensional case*

$$u^* = \arg \max_{\{u_i : i=0,\ldots,m-1\}} \left\{M_i^{P\theta}(u_i)\right\}$$

$$u_i = \max\left(\alpha_i, \min\left(\alpha_{i+1}, \frac{b - \bar{r} - r_i + \mu_i(1+\alpha_i)}{\Theta\sigma^2 + 2\mu_i}\right)\right)$$

2. Multidimensional case

$$u^* = \arg \max_{\{u_i : i=0,\dots,m-1\}} \left\{ M_i^{P\theta}(u_i) \right\}$$

for

$$u_i = \begin{cases} \frac{1}{\theta}(\sigma^*\sigma^{*\prime})^{-1} b^{*u} & : \quad v_i \notin \overline{D_i} \quad \wedge \quad \text{dist}(H_i, v_i) > \text{dist}(H_{i+1}, v_i) \\ v_i & : \quad v_i \in \overline{D_i} \\ \frac{1}{\theta}(\sigma^*\sigma^{*\prime})^{-1} b^{*d} & : \quad v_i \notin \overline{D_i} \quad \wedge \quad \text{dist}(H_i, v_i) < \text{dist}(H_{i+1}, v_i) \end{cases}$$

with

$$\begin{aligned} v_i &= (\Theta\sigma\sigma' + 2\mu_i \underline{1}\,\underline{1}')^{-1} \left(b - \underline{1}(\bar{r} - r_i + \mu_i(1+\alpha_i))\right) \\ M_i^{P\Theta}(u) &= (\bar{r} + r_i + \mu_i(u'\underline{1} - \alpha_i))(1 - u'\underline{1}) + u'b - \frac{1}{2}\Theta u'\sigma\sigma' u \end{aligned}$$

and $\sigma^* \in \mathbb{R}^{(n-1)\times(n-1)}$ *with* $\sigma^*_{ki} = \sigma_{ki} - \sigma_{ni}$ *and* $b^{*u}_k = b_k - b_n - \theta\alpha_{i+1}\sum_{i=1}^n \sigma_{ni}\sigma^*_{ki}$ *resp.* $b^{*d}_k = b_k - b_n - \theta\alpha_i \sum_{i=1}^n \sigma_{ni}\sigma^*_{ki}$.

Proof: Again, due to Theorem 1 and Proposition 1, the optimal control exists and is given by

$$\begin{aligned} \pi^*(.) \equiv u^* &= \arg \max_{x \in \mathbb{R}^n} M^{P\Theta}(x) \\ &= \arg \max_{u_i} M_i^{P\theta}(u_i) \text{ with } u_i = \arg \max_{u \in \overline{D_i}} M_i^{P\theta}(u), \end{aligned}$$

with $\Theta = 1$. Again, only the form of u_i has to be verified:

$$M_i^{P\Theta}(u) = (\bar{r} + r_i - \mu_i\alpha_i) + u'\big(b - \underline{1}(\bar{r} + r_i - \mu_i(1+\alpha_i))\big) - \frac{1}{2}u'(\Theta\sigma\sigma' + 2\mu_i\underline{1}\,\underline{1}')u$$

Because $M^{P\theta}$ is continuous, the above procedure is valid. More precisely, due to continuity, we have $\sup_{x\in U} M^{\theta}(x) = \max_i \sup_{x\in D_i} M_i^{S\theta}(x) = \max_i \max_{x\in\overline{D_i}} M_i^{S\theta}(x)$, and thus the above equation follows. Observe, that $\mu_i \underline{1}\,\underline{1}'$ is positive semidefinite, since $\mu_i > 0$ and $u'\underline{1}\,\underline{1}'u = (\sum_{i=1}^n u_i)^2 \geq 0$. Thus $\Theta\sigma\sigma' + 2\mu_i\underline{1}\,\underline{1}'$ is still strictly positive definite. So as before, we are concerned with downwards opening parabolas.

One-dimensional case
The argumentation is exactly the same as in the proof for step functions. But in contrast to the step function, we have to check all intervalls to get the maximum. More precisely, due to "strong" increasing slopes, it can happen that the apex lies in the interior of an intervall, but the absolute maximum lies in an intervall right from it.

Multidimensional case
Let $\Phi_i = \bar{r} + r_i - \mu_i\alpha_i$, $\Psi_i = \bar{r} + r_i - \mu_i(1+\alpha_i))$ and $M_i^{P\Theta}$ be the parabola on $\overline{D_i}$, i.e.:

$$M_i^{P\Theta}(u) = \left\{ \Phi_i + u'\big(b - \underline{1}\Psi_i\big) - \frac{1}{2}u'(\Theta\sigma\sigma' + 2\mu_i\underline{1}\,\underline{1}')u \right\} \tag{17}$$

The first step is to determine the apex without any restrictrictions on the domain.

$$\begin{aligned} v_i &:= \arg\max_{u\in I\!R^n} \left\{ \Phi_i + u'\big(b - \underline{1}\Psi_i\big) - \frac{1}{2}u'(\Theta\sigma\sigma' + 2\mu_i \underline{1}\,\underline{1}')u \right\} \\ &= (\Theta\sigma\sigma' + 2\mu_i \underline{1}\,\underline{1}')^{-1}\left(b - \underline{1}(\bar{r} - r_i + \mu_i(1+\alpha_i))\right) \end{aligned}$$

If $v_i \in \overline{D_i}$, then we have already found the local maximum and can define:

$$u_i = v_i$$

If $v_i \notin \overline{D_i}$, then the local maximum must lie in one of the hyperplanes H_i respectively H_{i+1}, since $-\sigma\sigma'$ is strictly negative definite and $M_i^{S\Theta}$ therefore strictly concave. If $\operatorname{dist}(H_i, v_i) > (<) \operatorname{dist}(H_{i+1}, v_i)$ then u_i lies in H_{i+1} (H_i). Thus we have to calculate the maximum under the constraint $v_i'\underline{1} = \alpha$, with $\alpha = \alpha_i$ resp. $\alpha = \alpha_{i+1}$ again.
As before we have to use the components of the vector u and b to do our calculations. Therefore, we will neglect the index i to avoid confusion:

$$\begin{aligned} v &= \arg\max_{u\in H} \left\{ \Phi + u'\big(b - \underline{1}\Psi\big) - \frac{1}{2}u'(\Theta\sigma\sigma' + 2\mu \underline{1}\,\underline{1}')u \right\} \\ &= \arg\max_{u\in I\!R^{n-1}} \left\{ \Phi + \sum_{k=1}^{n-1} u_k(b_k - \Psi) + (\alpha - \sum_{k=1}^{n-1} u_k)(b_n - \Psi) \right. \\ &\qquad \left. -\frac{1}{2}\Theta \sum_{i=1}^{n} \left(\sum_{k=1}^{n-1} u_k\sigma_{ki} + (\alpha - \sum_{k=1}^{n-1} u_k)\sigma_{ni} \right)^2 - \mu \underbrace{\left(\sum_{k=1}^{n-1} u_k + (\alpha - \sum_{k=1}^{n-1} u_k) \right)^2}_{=\alpha^2} \right\} \\ &= \arg\max_{u\in I\!R^{n-1}} \left\{ \Phi + \alpha(b_n - \Psi) - \mu\alpha^2 + \sum_{k=1}^{n-1} u_k(b_k - b_n) \right. \\ &\qquad \left. -\frac{1}{2}\Theta \sum_{i=1}^{n} \left(\sum_{k=1}^{n-1} u_k(\sigma_{ki} - \sigma_{ni}) + \alpha\sigma_{ni} \right)^2 \right\} \end{aligned}$$

As before let $b^* \in I\!R^{n-1}$ with $b_k^* = b_k - b_n$ and $\sigma^* \in I\!R^{(n-1)\times(n-1)}$ with $\sigma_{ki}^* = \sigma_{ki} - \sigma_{ni}$. Again we have $\operatorname{rank}(\sigma^*) = n-1$. Thus σ^* is regular and

$$\begin{aligned} v &= \arg\max_{u\in I\!R^{n-1}} \left\{ \Phi + \alpha(b_n - \Psi) - \mu\alpha^2 + \sum_{k=1}^{n-1} u_k b_k^* \right. \\ &\qquad \left. -\frac{1}{2}\Theta \sum_{i=1}^{n} \left(\left(\sum_{k=1}^{n-1} u_k\sigma_{ki}^* \right)^2 + 2\alpha\sigma_{ni} \sum_{k=1}^{n-1} u_k\sigma_{ki}^* + \alpha^2\sigma_{ni}^2 \right) \right\} \end{aligned}$$

$$v = \arg\max_{u\in\mathbb{R}^{n-1}} \left\{ \Phi + \alpha(b_n - \Psi) - \mu\alpha^2 - \frac{1}{2}\Theta\sum_{i=1}^{n}\alpha^2\sigma_{ni}^2 + \sum_{k=1}^{n-1} u_k \left(b_k^* - \Theta\alpha\sum_{i=1}^{n}\sigma_{ni}\sigma_{ki}^* \right) - \frac{1}{2}\Theta\sum_{i=1}^{n}\left(\left(\sum_{k=1}^{n-1} u_k\sigma_{ki}^* \right)^2 \right) \right\}$$

Thus, with $b_k^{**} = b_k^* - \Theta\alpha\sum_{i=1}^{n}\sigma_{ni}\sigma_{ki}^*$, we obtain the usual representation:

$$v = \arg\max_{u\in\mathbb{R}^{n-1}} \left\{ \Phi + \alpha(b_n - \Psi) - \mu\alpha^2 - \frac{1}{2}\Theta\sum_{i=1}^{n}\alpha^2\sigma_{ni}^2 + u'b^{**} - \frac{1}{2}\Theta u'\sigma^*\sigma^{*\prime}u \right\}$$

which yields the solution:

$$v = \frac{1}{\Theta}(\sigma^*\sigma^{*\prime})^{-1}b^{**}$$

It is wortwhile to note that the maximum does neither depend on the interest rate $\bar{r} + r_i$, nor on μ_i, and the calculation of the maximum is exactly the same as for step functions. This is not suprising, since r is fixed on these hyperplanes.

□

Example 2
Let $r(u)$ be modelled as in Figure 2, i.e.

$$r(u) = \begin{cases} 5\% & : \quad u \le 1 \\ 5\% + (u-1)*3\% & : \quad 1 < u \le 1.5 \\ 6.5\% + (u-1.5)*6\% & : \quad 1.5 < u \le 2 \\ 9.5\% + (u-2)*3\% & : \quad 2 < u \le 2.5 \\ 11\% & : \quad 2.5 < u \end{cases},$$

Let $b = 12\%$ and $\sigma = 20\%$, then the optimal control equals $\pi^*(.) = \frac{12\%-5\%+3\%*2}{20\%^2+2*3\%} = 1.3$. For comparison: If $r(u) \equiv 5\%$ then again the optimal control equals 1.75.

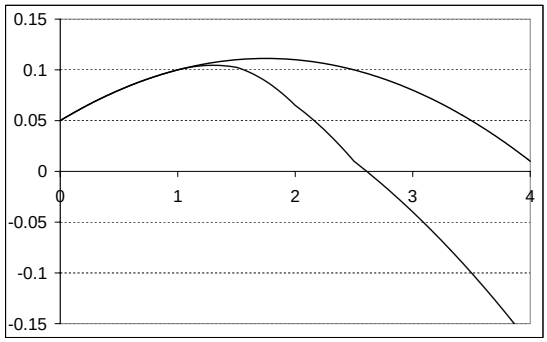

Figure 5: Parabolas M^{P1} with r frequency polygon and flat

Note that the parabola is generally not differentiable in the α_i.

3.3 Logistic function

The optimal control ist given by:

$$\hat{\pi}^*(t) \quad = \quad \arg\max_u \left\{ \left[\bar{r} \; + \lambda \frac{e^{\alpha u' \underline{1} + \beta}}{e^{\alpha' u \underline{1} + \beta} + 1} \right] (1 - u' \underline{1}) + u' b \; - \frac{1}{2} u' \sigma \sigma' u \right\}$$

Since $r(u)$ is bounded we get, very loosely speaking, a kind of downwards opened parabola. Thus, surely there exists an absolute maximum. In the one-dimensional case we have to solve the following equation:

$$\underbrace{(1-u)\lambda \frac{\alpha e^{\alpha u+\beta}}{(e^{\alpha u+\beta}+1)^2}}_{A(u)} - \underbrace{\lambda \frac{\alpha e^{\alpha u+\beta}}{e^{\alpha u+\beta}+1}}_{B(u)} \stackrel{!}{=} u\sigma^2 - b + \bar{r}$$

Since $\lim_{u\to\infty} A(u) = 0$,$\lim_{u\to-\infty} A(u) = 0$, A(u) is bounded. In conjunction with the boundness of B(u) and continuity we can infer that the above equation has a solution u^*. This can be determined by a simple Newton algorithm. Because $\pi^*(t) \equiv u^*$ is constant, it belongs to $\mathcal{A}(0, x_0)$. As before it follows, that the original optimisation problem is solved too.

Example 3
Let $r(u)$ be modelled as in Figure 3, i.e. $\bar{r} = 5\%$, $\lambda = 6\%$, $\alpha = 3$ and $\beta = 4$. Then the optimal control is 1.26.

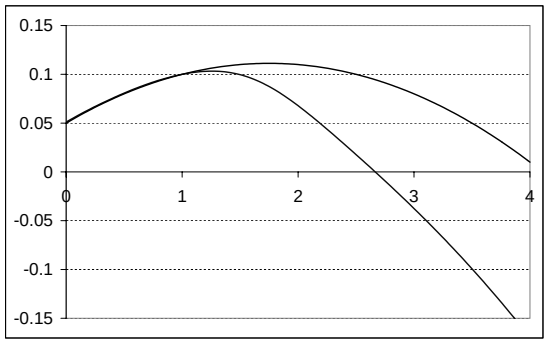

Figure 6: Parabolas with r logistic function and flat

4 Power Utility

Let $U(x) = \frac{1}{\gamma} x^\gamma$ with $\gamma \in (-\infty, 0) \cup (0, 1)$ then with (2) and (3) we get the following optimisation problem:

$$V(t,x) \quad := \quad \frac{1}{\gamma} \sup_{\pi(.)\in\mathcal{A}(t,x)} E^{t,x}((X^\pi(T))^\gamma) \tag{18}$$

$$= \quad \frac{1}{\gamma} \sup_{\pi(.)\in\mathcal{A}(t,x)} \left\{ x^\gamma E e^{\gamma \left[\int_t^T \left(r(\pi(t))(1-\pi'(t)\underline{1}) + \pi'(t) b - \frac{1}{2}\pi'(t)\sigma\sigma'\pi(t) \right) dt + \int_t^T \pi(t)\sigma dW(t) \right]} \right\}$$

Again, this optimisation problem is solved by a pointwise maximization. But, due to the non-linear structure of the above term, the correctness cannot be shown by some simple inequaltities as in the logarithmic case. Instead of this, will show the correnctness via the verification theorem in Korn and Korn (2001):

Theorem 4 : Verification with power utility
The value function with power utility is given by:

$$V(t,x) = \frac{1}{\gamma} x^\gamma e^{\gamma\left[(r(u^*)(1-u^{*\prime}\underline{1})+u^{*\prime}b-\frac{1}{2}(1-\gamma)u^{*\prime}\sigma\sigma^\prime u^*\right](T-t)}$$

and the optimal control exists and is given by:

$$\pi^*(.) \equiv u^* = \arg\max_u \left[r(u)(1-u^\prime\underline{1}) + u^\prime b - \frac{1}{2}(1-\gamma)u^\prime\sigma\sigma^\prime u \right]$$

Proof: The existence of the maximum was already shown in Proposition 1. So it is left, to check the conditions of the verification theorem in Korn and Korn (2001). Let:

$$G^{u^*}(t,x) = \frac{1}{\gamma} x^\gamma e^{\gamma\left[(r(u^*)(1-u^{*\prime}\underline{1})+u^{*\prime}b-\frac{1}{2}(1-\gamma)u^{*\prime}\sigma\sigma^\prime u^*\right](T-t)}$$

The function $G^{u^*}(t,x)$ is sufficiently smooth and polynomially bounded. In addition, we have to show:

$$\sup_{u\in\mathbb{R}^+} \left(\mathcal{A}^u(G^{u^*}(t,x))\right) = 0\,,$$

where

$$\mathcal{A}^u = \frac{\partial}{\partial t} + \left[r(u)(1-u^\prime\underline{1}) + u^\prime b\right] x\frac{\partial}{\partial x} + \frac{1}{2}u^\prime\sigma\sigma^\prime u x^2\frac{\partial^2}{\partial^2 x}\,.$$

As we can easily verify $\mathcal{A}^{u^*}(G^{u^*}(t,x)) = 0$, we only have to show that there does not exist an $u \neq u^*$ such that:

$$A^u(G^{u^*}(t,x)) > 0$$

But this leads to:

$$\left(\frac{\partial}{\partial t} + \left[r(u)(1-u^\prime\underline{1}) + u^\prime b\right] x\frac{\partial}{\partial x} + \frac{1}{2}u^\prime\sigma\sigma^\prime u x^2\frac{\partial^2}{\partial^2 x}\right) G^{u^*}(t,x) > 0$$

$$\Leftrightarrow \quad \frac{1}{\gamma} e^{\gamma\left[r(u^*)(1-u^{*\prime}\underline{1})+u^{*\prime}b-\frac{1}{2}(1-\gamma)u^{*\prime}\sigma\sigma^\prime u^*\right](T-t)} \Bigg\{ -x^\lambda\gamma\Bigg[r(u^*)(1-u^{*\prime}\underline{1}) + u^{*\prime}$$

$$-\frac{1}{2}(1-\gamma)u^{*\prime}\sigma\sigma^\prime u^*\Bigg] + \left[r(u)(1-u^\prime\underline{1}) + u^\prime b\right] x\gamma x^{\gamma-1} + \frac{1}{2}u^\prime\sigma\sigma^\prime u x^2\gamma(\gamma-1)x^{\gamma-2}\Bigg\} > 0$$

$$\Leftrightarrow \quad r(u)(1-u^\prime\underline{1}) + u^\prime b - \frac{1}{2}(1-\gamma)u^\prime\sigma\sigma^\prime u > r(u^*)(1-u^{*\prime}\underline{1}) + u^{*\prime}b - \frac{1}{2}(1-\gamma)u^{*\prime}\sigma\sigma^\prime u^*$$

which contradicts the construction of u^*, and thus, the assertion follows. Verification is now completed by also noting $G^{u^*}(T,x) = \frac{1}{\gamma}x^\gamma$. □

As in the case with logarithmic utility the optimisation problem is reduced to the maximisation of downwards opening parabolas. Hence, the further steps will be very similar.

4.1 Step function

Theorem 5 : Optimal Portfolios with step functions and power utility

Let $V^S(t,x)$ be the value function given in (18) with $r(u)$ step function defined by (4). In addition, let $M^{S(1-\gamma)}$ be the corresponding function to be maximised in Proposition 1 with $r(u)$ step function i.e.:

$$M^{S(1-\gamma)} = \left[\bar{r} + \sum_{i=0}^{n-1} \lambda_i \mathbf{1}_{(\alpha_i,\alpha_{i+1}]}(u'\underline{1})\right](1-u'\underline{1}) + u'b - \frac{1}{2}\Theta u'\sigma\sigma' u$$

with α_i, λ_i given in (4). Then there exists an optimal (constant) control $\pi^*(.) = u^* = \arg\max_{u\in\mathbb{R}^n} M^{S(1-\gamma)}(u)$ such that

$$V^S(t,x) \equiv \sup_{\pi(.)\in\mathcal{A}(t,x)} E^{t,x}\left(\frac{1}{\gamma}(X^{\pi}(T))^{\gamma}\right) = E^{t,x}\left(\frac{1}{\gamma}(X^{\pi^*}(T))^{\gamma}\right) \quad .$$

The number u^* is explicitly given in Theorem 2 with $\Theta = (1-\gamma)$.

PROOF: The existence of the maximum was shown in Proposition 1. The correctness of the value function was proved in Theorem 4. The determination of u^* is exactly the same as in Theorem 2. □

Example 4

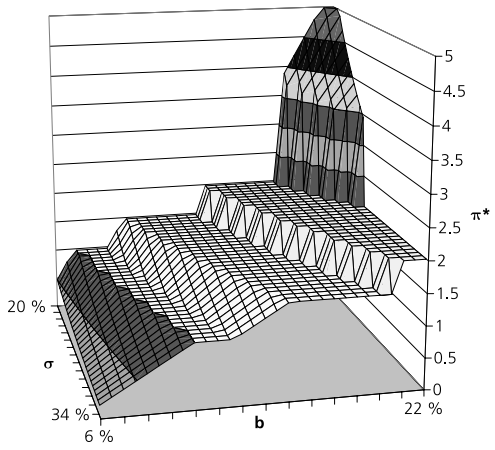

Figure 7: Optimal control with $r(.)$ step function and power utility ($\gamma = 0.5$)

In Figure 7 we observe the well known and natural result, that the optimal control π^* increases when the asset drift increases resp. the volatility decreases. But there is a new feature: There are plateaus on levels which equal the points of discontinuity of $r(u)$, i.e. α_i. On these regions it is not benefitial to increase π when the stock drift (slightly) increases, because the loss due to the more expensive payments of interest (via the upwards-jump of $r(\pi)$) is higher than the benefit due to the higher position in the stock. Conversely, it is not benefitial, to reduce the stock positions, when b (slightly) decreases, because r would not

fall, and thus the gain from decreasing interest payments would not be higher than the loss via the shortage of the stock-position. If the drift is strongly changing the above effects beat their counterparts, and the optimal control is jumping to the next plateau. In $\alpha_1 = 1$ there is no jump, because the parabola is continuous at this point, as explained before.

4.2 Polygon frequency

Theorem 6 : Optimal Portfolios with polygons and power utility

Let $V^P(t,x)$ be the value function given in (18) with $r(u)$ frequency polygon defined by (5). In addition, let $M^{P(1-\gamma)}$ be the corresponding function to be maximised in Proposition 1 with $r(u)$ frequency polygon i.e.:

$$M^{P(1-\gamma)}(u) \quad = \quad \left[\bar{r} \; + \sum_{i=0}^{n-1} \left[(r_i + \mu_i(u'\underline{1} - \alpha_i))\right] \mathbf{1}_{[\alpha_i,\alpha_{i+1})}(u'\underline{1})\right](1 - u'\underline{1}) + u'b - \frac{1}{2}(1-\gamma)u'\sigma\sigma'u$$

with α_i, μ_i, r_i given in (5). then there exists a constant control $\pi^*(.) = u^* = \arg\max_{u \in I\!R^n} M^{P\theta}(u)$ such that

$$V^P(t,x) \equiv \sup_{\pi(.)\in\mathcal{A}(t,x)} E^{t,x}\left(\frac{1}{\gamma}(X^{\pi}(T))^{\gamma}\right) = E^{t,x}\left(\frac{1}{\gamma}(X^{\pi^*}(T))^{\gamma}\right) \quad .$$

The number u^* is explicitly given in Theorem 3 with $\Theta = (1-\gamma)$.

PROOF: The existence of the maximum was shown in Proposition 1. The correctness of the value function was proved in Theorem 4. The determination of u^* is exactly the same as in Theorem 3. □

Example 5

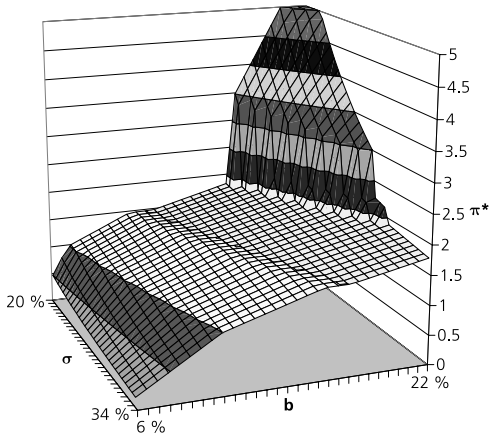

Figure 8: Optimal control with r(u) frequency polygon and power utility ($\gamma = 0.50$)

Again, we observe the obvious behavior, that the optimal control π^* increases when the asset drift increases resp. the volatility decreases. But on the points of discontinuity of the first

derivative, i.e. α_i, there are different properties: In $\alpha_1 = 1.0$ there is a sharp bend on the surface, instead of a plateau. In $\alpha_2 = 1.5$ there is again a small plateau. Then π is slightly increasing between 1.5 and 2.5 and then it jumps to a value at 3.5.

5 Conclusions

Optimal control for other dependencies
Note that in the case of frequency polygons, the value function is a continuous function from the space of frequency polygons to the real numbers, because the apex and the maximum function is continuous. Let $\tilde{r}(u) : \mathbb{R}^n \to \mathbb{R}$ be a a bounded and continuously differentiable function. Since $\tilde{r}(u)$ is bounded and continuous, the maximum of the corresponding function $M^\theta(x)$ in Proposition 1, and thus a optimal control u^* exists. We can restrict the domain of $\tilde{r}(u)$ on a compact set, which is sufficiently large, such that u^* lies in it. On this compact set $\tilde{r}(u)$ can be uniformely approximated by a sequence of frequency polygons $P_n(u)$, i.e. $\|P_n(.) - \tilde{r}(.)\| \to 0$. Hence via the above noted continuity we obtain

$$E^{t,x}\left[U\left(X^{\pi^{*,P_n(.)}}\right)\right] \to E^{t,x}\left[U\left(X^{\pi^{*,\tilde{r}(.)}}\right)\right]$$

where U equals log or power utility and $\pi^{*,f(.)}$ denotes the optimal control with control depending interest rate $r(t) = f(\pi(t))$. Unfortunately, the optimal control does not necessarily converge, because 'arg max' is not continuous. But if π^* is unique (that means the difference between the absolute maximum and nearest local maximum is greater than zero), we obtain convergence of the control too, because $\pi^{*,P_n(.)}$ cannot alternate between to local maxima, if n is sufficiently high.

Closing remarks
We showed that a control-depending interest rate can be easily included into portfolio optimisation. We provided explicit solutions for step functions and frequency polygons in the both cases logarithmic and power utility. In addition we showed convergence of the optimal control; a feature, which is generally hard to obtain in portfolio optimisation. Independent from credit risk, this method can also be used to avoid high controls, in a sense of an implicit risk controlling.

References

Korn R. (1995): "Contingent Claim Valuation with Different Interest Rates", *Zeitschrift für Operations Research*, Vol. 42, Issue 3, S. 255-264.

Korn R., Korn E. (2001): *Option pricing and portfolio optimisation*, AMS.

Korn R., Wilmott P. (2000): *Optimal investment under a threat of crash* , to appear in: ISTAF.

Merton, Robert C. (1969): "Lifetime Portfolio Selection under Uncertainty: The Continuous-Time Case", *Review of Economics and Statistics* , Vol. 51, S. 247-257.

Merton, Robert C. (1971): "Optimum Consumption and Portfolio Rules in a Continuous-Time Model", *Journal of Economic Theory*, Vol. 3, S. 373-413.

Bisher erschienene Berichte des Fraunhofer ITWM

Die PDF-Files der folgenden Berichte finden Sie unter:
www.itwm.fhg.de/zentral/berichte.html

1. D. Hietel, K. Steiner, J. Struckmeier

A Finite - Volume Particle Method for Compressible Flows

We derive a new class of particle methods for conservation laws, which are based on numerical flux functions to model the interactions between moving particles. The derivation is similar to that of classical Finite-Volume methods; except that the fixed grid structure in the Finite-Volume method is substituted by so-called mass packets of particles. We give some numerical results on a shock wave solution for Burgers equation as well as the well-known one-dimensional shock tube problem.
(19 S., 1998)

2. M. Feldmann, S. Seibold

Damage Diagnosis of Rotors: Application of Hilbert Transform and Multi-Hypothesis Testing

In this paper, a combined approach to damage diagnosis of rotors is proposed. The intention is to employ signal-based as well as model-based procedures for an improved detection of size and location of the damage. In a first step, Hilbert transform signal processing techniques allow for a computation of the signal envelope and the instantaneous frequency, so that various types of non-linearities due to a damage may be identified and classified based on measured response data. In a second step, a multi-hypothesis bank of Kalman Filters is employed for the detection of the size and location of the damage based on the information of the type of damage provided by the results of the Hilbert transform.
Keywords:
Hilbert transform, damage diagnosis, Kalman filtering, non-linear dynamics
(23 S., 1998)

3. Y. Ben-Haim, S. Seibold

Robust Reliability of Diagnostic Multi-Hypothesis Algorithms: Application to Rotating Machinery

Damage diagnosis based on a bank of Kalman filters, each one conditioned on a specific hypothesized system condition, is a well recognized and powerful diagnostic tool. This multi-hypothesis approach can be applied to a wide range of damage conditions. In this paper, we will focus on the diagnosis of cracks in rotating machinery. The question we address is: how to optimize the multi-hypothesis algorithm with respect to the uncertainty of the spatial form and location of cracks and their resulting dynamic effects. First, we formulate a measure of the reliability of the diagnostic algorithm, and then we discuss modifications of the diagnostic algorithm for the maximization of the reliability. The reliability of a diagnostic algorithm is measured by the amount of uncertainty consistent with no-failure of the diagnosis. Uncertainty is quantitatively represented with convex models.
Keywords:
Robust reliability, convex models, Kalman filtering, multi-hypothesis diagnosis, rotating machinery, crack diagnosis
(24 S., 1998)

4. F.-Th. Lentes, N. Siedow

Three-dimensional Radiative Heat Transfer in Glass Cooling Processes

For the numerical simulation of 3D radiative heat transfer in glasses and glass melts, practically applicable mathematical methods are needed to handle such problems optimal using workstation class computers. Since the exact solution would require super-computer capabilities we concentrate on approximate solutions with a high degree of accuracy. The following approaches are studied: 3D diffusion approximations and 3D ray-tracing methods.
(23 S., 1998)

5. A. Klar, R. Wegener

A hierarchy of models for multilane vehicular traffic
Part I: Modeling

In the present paper multilane models for vehicular traffic are considered. A microscopic multilane model based on reaction thresholds is developed. Based on this model an Enskog like kinetic model is developed. In particular, care is taken to incorporate the correlations between the vehicles. From the kinetic model a fluid dynamic model is derived. The macroscopic coefficients are deduced from the underlying kinetic model. Numerical simulations are presented for all three levels of description in [10]. Moreover, a comparison of the results is given there.
(23 S., 1998)

Part II: Numerical and stochastic investigations

In this paper the work presented in [6] is continued. The present paper contains detailed numerical investigations of the models developed there. A numerical method to treat the kinetic equations obtained in [6] are presented and results of the simulations are shown. Moreover, the stochastic correlation model used in [6] is described and investigated in more detail.
(17 S., 1998)

6. A. Klar, N. Siedow

Boundary Layers and Domain Decomposition for Radiative Heat Transfer and Diffusion Equations: Applications to Glass Manufacturing Processes

In this paper domain decomposition methods for radiative transfer problems including conductive heat transfer are treated. The paper focuses on semi-transparent materials, like glass, and the associated conditions at the interface between the materials. Using asymptotic analysis we derive conditions for the coupling of the radiative transfer equations and a diffusion approximation. Several test cases are treated and a problem appearing in glass manufacturing processes is computed. The results clearly show the advantages of a domain decomposition approach. Accuracy equivalent to the solution of the global radiative transfer solution is achieved, whereas computation time is strongly reduced.
(24 S., 1998)

7. I. Choquet

Heterogeneous catalysis modelling and numerical simulation in rarified gas flows Part I: Coverage locally at equilibrium

A new approach is proposed to model and simulate numerically heterogeneous catalysis in rarefied gas flows. It is developed to satisfy all together the following points:
1) describe the gas phase at the microscopic scale, as required in rarefied flows,
2) describe the wall at the macroscopic scale, to avoid prohibitive computational costs and consider not only crystalline but also amorphous surfaces,
3) reproduce on average macroscopic laws correlated with experimental results and
4) derive analytic models in a systematic and exact way.
The problem is stated in the general framework of a non static flow in the vicinity of a catalytic and non porous surface (without aging). It is shown that the exact and systematic resolution method based on the Laplace transform, introduced previously by the author to model collisions in the gas phase, can be extended to the present problem. The proposed approach is applied to the modelling of the Eley-Rideal and Langmuir-Hinshelwood recombinations, assuming that the coverage is locally at equilibrium. The models are developed considering one atomic species and extended to the general case of several atomic species. Numerical calculations show that the models derived in this way reproduce with accuracy behaviors observed experimentally.
(24 S., 1998)

8. J. Ohser, B. Steinbach, C. Lang

Efficient Texture Analysis of Binary Images

A new method of determining some characteristics of binary images is proposed based on a special linear filtering. This technique enables the estimation of the area fraction, the specific line length, and the specific integral of curvature. Furthermore, the specific length of the total projection is obtained, which gives detailed information about the texture of the image. The influence of lateral and directional resolution depending on the size of the applied filter mask is discussed in detail. The technique includes a method of increasing directional resolution for texture analysis while keeping lateral resolution as high as possible.
(17 S., 1998)

9. J. Orlik

Homogenization for viscoelasticity of the integral type with aging and shrinkage

A multi-phase composite with periodic distributed inclusions with a smooth boundary is considered in this contribution. The composite component materials are supposed to be linear viscoelastic and aging (of the non-convolution integral type, for which the Laplace transform with respect to time is not effectively applicable) and are subjected to isotropic shrinkage. The free shrinkage deformation can be considered as a fictitious temperature deformation in the behavior law. The procedure presented in this paper proposes a way to determine average (effective homogenized) viscoelastic and shrinkage (temperature) composite properties and the homogenized stress-field from known properties of the

components. This is done by the extension of the asymptotic homogenization technique known for pure elastic non-homogeneous bodies to the non-homogeneous thermo-viscoelasticity of the integral non-convolution type. Up to now, the homogenization theory has not covered viscoelasticity of the integral type.
Sanchez-Palencia (1980), Francfort & Suquet (1987) (see [2], [9]) have considered homogenization for viscoelasticity of the differential form and only up to the first derivative order. The integral-modeled viscoelasticity is more general then the differential one and includes almost all known differential models. The homogenization procedure is based on the construction of an asymptotic solution with respect to a period of the composite structure. This reduces the original problem to some auxiliary boundary value problems of elasticity and viscoelasticity on the unit periodic cell, of the same type as the original non-homogeneous problem. The existence and uniqueness results for such problems were obtained for kernels satisfying some constrain conditions. This is done by the extension of the Volterra integral operator theory to the Volterra operators with respect to the time, whose 1 kernels are space linear operators for any fixed time variables. Some ideas of such approach were proposed in [11] and [12], where the Volterra operators with kernels depending additionally on parameter were considered. This manuscript delivers results of the same nature for the case of the space-operator kernels.
(20 S., 1998)

10. J. Mohring

Helmholtz Resonators with Large Aperture

The lowest resonant frequency of a cavity resonator is usually approximated by the classical Helmholtz formula. However, if the opening is rather large and the front wall is narrow this formula is no longer valid. Here we present a correction which is of third order in the ratio of the diameters of aperture and cavity. In addition to the high accuracy it allows to estimate the damping due to radiation. The result is found by applying the method of matched asymptotic expansions. The correction contains form factors describing the shapes of opening and cavity. They are computed for a number of standard geometries. Results are compared with numerical computations.
(21 S., 1998)

11. H. W. Hamacher, A. Schöbel

On Center Cycles in Grid Graphs

Finding "good" cycles in graphs is a problem of great interest in graph theory as well as in locational analysis. We show that the center and median problems are NP hard in general graphs. This result holds both for the variable cardinality case (i.e. all cycles of the graph are considered) and the fixed cardinality case (i.e. only cycles with a given cardinality p are feasible). Hence it is of interest to investigate special cases where the problem is solvable in polynomial time.
In grid graphs, the variable cardinality case is, for instance, trivially solvable if the shape of the cycle can be chosen freely.
If the shape is fixed to be a rectangle one can analyze rectangles in grid graphs with, in sequence, fixed dimension, fixed cardinality, and variable cardinality. In all cases a complete characterization of the optimal cycles and closed form expressions of the optimal objective values are given, yielding polynomial time algorithms for all cases of center rectangle problems.
Finally, it is shown that center cycles can be chosen as rectangles for small cardinalities such that the center cycle problem in grid graphs is in these cases completely solved.
(15 S., 1998)

12. H. W. Hamacher, K.-H. Küfer

Inverse radiation therapy planning - a multiple objective optimisation approach

For some decades radiation therapy has been proved successful in cancer treatment. It is the major task of clinical radiation treatment planning to realize on the one hand a high level dose of radiation in the cancer tissue in order to obtain maximum tumor control. On the other hand it is obvious that it is absolutely necessary to keep in the tissue outside the tumor, particularly in organs at risk, the unavoidable radiation as low as possible.
No doubt, these two objectives of treatment planning - high level dose in the tumor, low radiation outside the tumor - have a basically contradictory nature. Therefore, it is no surprise that inverse mathematical models with dose distribution bounds tend to be infeasible in most cases. Thus, there is need for approximations compromising between overdosing the organs at risk and underdosing the target volume.
Differing from the currently used time consuming iterative approach, which measures deviation from an ideal (non-achievable) treatment plan using recursively trial-and-error weights for the organs of interest, we go a new way trying to avoid a priori weight choices and consider the treatment planning problem as a multiple objective linear programming problem: with each organ of interest, target tissue as well as organs at risk, we associate an objective function measuring the maximal deviation from the prescribed doses.
We build up a data base of relatively few efficient solutions representing and approximating the variety of Pareto solutions of the multiple objective linear programming problem. This data base can be easily scanned by physicians looking for an adequate treatment plan with the aid of an appropriate online tool.
(14 S., 1999)

13. C. Lang, J. Ohser, R. Hilfer

On the Analysis of Spatial Binary Images

This paper deals with the characterization of microscopically heterogeneous, but macroscopically homogeneous spatial structures. A new method is presented which is strictly based on integral-geometric formulae such as Crofton's intersection formulae and Hadwiger's recursive definition of the Euler number. The corresponding algorithms have clear advantages over other techniques. As an example of application we consider the analysis of spatial digital images produced by means of Computer Assisted Tomography.
(20 S., 1999)

14. M. Junk

On the Construction of Discrete Equilibrium Distributions for Kinetic Schemes

A general approach to the construction of discrete equilibrium distributions is presented. Such distribution functions can be used to set up Kinetic Schemes as well as Lattice Boltzmann methods. The general principles are also applied to the construction of Chapman Enskog distributions which are used in Kinetic Schemes for compressible Navier-Stokes equations.
(24 S., 1999)

15. M. Junk, S. V. Raghurame Rao

A new discrete velocity method for Navier-Stokes equations

The relation between the Lattice Boltzmann Method, which has recently become popular, and the Kinetic Schemes, which are routinely used in Computational Fluid Dynamics, is explored. A new discrete velocity model for the numerical solution of Navier-Stokes equations for incompressible fluid flow is presented by combining both the approaches. The new scheme can be interpreted as a pseudo-compressibility method and, for a particular choice of parameters, this interpretation carries over to the Lattice Boltzmann Method.
(20 S., 1999)

16. H. Neunzert

Mathematics as a Key to Key Technologies

The main part of this paper will consist of examples, how mathematics really helps to solve industrial problems; these examples are taken from our Institute for Industrial Mathematics, from research in the Technomathematics group at my university, but also from ECMI groups and a company called TecMath, which originated 10 years ago from my university group and has already a very successful history.
(39 S. (vier PDF-Files), 1999)

17. J. Ohser, K. Sandau

Considerations about the Estimation of the Size Distribution in Wicksell's Corpuscle Problem

Wicksell's corpuscle problem deals with the estimation of the size distribution of a population of particles, all having the same shape, using a lower dimensional sampling probe. This problem was originary formulated for particle systems occurring in life sciences but its solution is of actual and increasing interest in materials science. From a mathematical point of view, Wicksell's problem is an inverse problem where the interesting size distribution is the unknown part of a Volterra equation. The problem is often regarded ill-posed, because the structure of the integrand implies unstable numerical solutions. The accuracy of the numerical solutions is considered here using the condition number, which allows to compare different numerical methods with different (equidistant) class sizes and which indicates, as one result, that a finite section thickness of the probe reduces the numerical problems. Furthermore, the relative error of estimation is computed which can be split into two parts. One part consists of the relative discretization error that increases for increasing class size, and the second part is related to the relative statistical error which increases with decreasing class size. For both parts, upper bounds can be given and the sum of them indicates an optimal class width depending on some specific constants.
(18 S., 1999)

18. E. Carrizosa, H. W. Hamacher, R. Klein, S. Nickel

Solving nonconvex planar location problems by finite dominating sets

It is well-known that some of the classical location problems with polyhedral gauges can be solved in polynomial time by finding a finite dominating set, i. e. a finite set of candidates guaranteed to contain at least one optimal location.
In this paper it is first established that this result holds for a much larger class of problems than currently considered in the literature. The model for which this result can be proven includes, for instance, location problems with attraction and repulsion, and location-allocation problems. Next, it is shown that the approximation of general gauges by polyhedral ones in the objective function of our general model can be analyzed with regard to the subsequent error in the optimal objective value. For the approximation problem two different approaches are described, the sandwich procedure and the greedy algorithm. Both of these approaches lead - for fixed epsilon - to polynomial approximation algorithms with accuracy epsilon for solving the general model considered in this paper.
Keywords:
Continuous Location, Polyhedral Gauges, Finite Dominating Sets, Approximation, Sandwich Algorithm, Greedy Algorithm
(19 S., 2000)

19. A. Becker

A Review on Image Distortion Measures

Within this paper we review image distortion measures. A distortion measure is a criterion that assigns a "quality number" to an image. We distinguish between mathematical distortion measures and those distortion measures in-cooperating a priori knowledge about the imaging devices (e. g. satellite images), image processing algorithms or the human physiology. We will consider representative examples of different kinds of distortion measures and are going to discuss them.
Keywords:
Distortion measure, human visual system
(26 S., 2000)

20. H. W. Hamacher, M. Labbé, S. Nickel, T. Sonneborn

Polyhedral Properties of the Uncapacit*ated Multiple Allocation Hub Location Problem*

We examine the feasibility polyhedron of the uncapacitated hub location problem (UHL) with multiple allocation, which has applications in the fields of air passenger and cargo transportation, telecommunication and postal delivery services. In particular we determine the dimension and derive some classes of facets of this polyhedron. We develop some general rules about lifting facets from the uncapacitated facility location (UFL) for UHL and projecting facets from UHL to UFL. By applying these rules we get a new class of facets for UHL which dominates the inequalities in the original formulation. Thus we get a new formulation of UHL whose constraints are all facet–defining. We show its superior computational performance by benchmarking it on a well known data set.
Keywords:
integer programming, hub location, facility location, valid inequalities, facets, branch and cut
(21 S., 2000)

21. H. W. Hamacher, A. Schöbel

Design of Zone Tariff Systems in Public Transportation

Given a public transportation system represented by its stops and direct connections between stops, we consider two problems dealing with the prices for the customers: The fare problem in which subsets of stops are already aggregated to zones and "good" tariffs have to be found in the existing zone system. Closed form solutions for the fare problem are presented for three objective functions. In the zone problem the design of the zones is part of the problem. This problem is NP hard and we therefore propose three heuristics which prove to be very successful in the redesign of one of Germany's transportation systems.
(30 S., 2001)

22. D. Hietel, M. Junk, R. Keck, D. Teleaga:

The Finite-Volume-Particle Method for Conservation Laws

In the Finite-Volume-Particle Method (FVPM), the weak formulation of a hyperbolic conservation law is discretized by restricting it to a discrete set of test functions. In contrast to the usual Finite-Volume approach, the test functions are not taken as characteristic functions of the control volumes in a spatial grid, but are chosen from a partition of unity with smooth and overlapping partition functions (the particles), which can even move along prescribed velocity fields. The information exchange between particles is based on standard numerical flux functions. Geometrical information, similar to the surface area of the cell faces in the Finite-Volume Method and the corresponding normal directions are given as integral quantities of the partition functions.
After a brief derivation of the Finite-Volume-Particle Method, this work focuses on the role of the geometric coefficients in the scheme.
(16 S., 2001)

23. T. Bender, H. Hennes, J. Kalcsics, M. T. Melo, S. Nickel

Location Software and Interface with GIS and Supply Chain Management

The objective of this paper is to bridge the gap between location theory and practice. To meet this objective focus is given to the development of software capable of addressing the different needs of a wide group of users. There is a very active community on location theory encompassing many research fields such as operations research, computer science, mathematics, engineering, geography, economics and marketing. As a result, people working on facility location problems have a very diverse background and also different needs regarding the software to solve these problems. For those interested in non-commercial applications (e. g. students and researchers), the library of location algorithms (LoLA can be of considerable assistance. LoLA contains a collection of efficient algorithms for solving planar, network and discrete facility location problems. In this paper, a detailed description of the functionality of LoLA is presented. In the fields of geography and marketing, for instance, solving facility location problems requires using large amounts of demographic data. Hence, members of these groups (e. g. urban planners and sales managers) often work with geographical information too s. To address the specific needs of these users, LoLA was inked to a geographical information system (GIS) and the details of the combined functionality are described in the paper. Finally, there is a wide group of practitioners who need to solve large problems and require special purpose software with a good data interface. Many of such users can be found, for example, in the area of supply chain management (SCM). Logistics activities involved in strategic SCM include, among others, facility location planning. In this paper, the development of a commercial location software tool is also described. The too is embedded in the Advanced Planner and Optimizer SCM software developed by SAP AG, Walldorf, Germany. The paper ends with some conclusions and an outlook to future activities.
Keywords:
facility location, software development, geographical information systems, supply chain management.
(48 S., 2001)

24. H. W. Hamacher, S. A. Tjandra

Mathematical Modelling of Evacuation Problems: A State of Art

This paper details models and algorithms which can be applied to evacuation problems. While it concentrates on building evacuation many of the results are applicable also to regional evacuation. All models consider the time as main parameter, where the travel time between components of the building is part of the input and the overall evacuation time is the output. The paper distinguishes between macroscopic and microscopic evacuation models both of which are able to capture the evacuees' movement over time.
Macroscopic models are mainly used to produce good lower bounds for the evacuation time and do not consider any individual behavior during the emergency situation. These bounds can be used to analyze existing buildings or help in the design phase of planning a building. Macroscopic approaches which are based on dynamic network flow models (minimum cost dynamic flow, maximum dynamic flow, universal maximum flow, quickest path and quickest flow) are described. A special feature of the presented approach is the fact, that travel times of evacuees are not restricted to be constant, but may be density dependent. Using multicriteria optimization priority regions and blockage due to fire or smoke may be considered. It is shown how the modelling can be done using time parameter either as discrete or continuous parameter.
Microscopic models are able to model the individual evacuee's characteristics and the interaction among evacuees which influence their movement. Due to the corresponding huge amount of data one uses simulation approaches. Some probabilistic laws for individual evacuee's movement are presented. Moreover ideas to model the evacuee's movement using cellular automata (CA) and resulting software are presented.
In this paper we will focus on macroscopic models and only summarize some of the results of the microscopic approach. While most of the results are applicable to general evacuation situations, we concentrate on building evacuation.
(44 S., 2001)

25. J. Kuhnert, S. Tiwari

Grid free method for solving the Poisson equation

A Grid free method for solving the Poisson equation is presented. This is an iterative method. The method is based on the weighted least squares approximation in which the Poisson equation is enforced to be satisfied in every iterations. The boundary conditions can also be enforced in the iteration process. This is a local approximation procedure. The Dirichlet, Neumann and mixed boundary value problems on a unit square are presented and the analytical solutions are compared with the exact solutions. Both solutions matched perfectly.
Keywords:
Poisson equation, Least squares method, Grid free method
(19 S., 2001)

26. T. Götz, H. Rave, D. Reinel-Bitzer, K. Steiner, H. Tiemeier

Simulation of the fiber spinning process

To simulate the influence of process parameters to the melt spinning process a fiber model is used and coupled with CFD calculations of the quench air flow. In the fiber model energy, momentum and mass balance are solved for the polymer mass flow. To calculate the quench air the Lattice Boltzmann method is used. Simulations and experiments for different process parameters and hole configurations are compared and show a good agreement.
Keywords:
Melt spinning, fiber model, Lattice Boltzmann, CFD
(19 S., 2001)

27. A. Zemitis

On interaction of a liquid film with an obstacle

In this paper mathematical models for liquid films generated by impinging jets are discussed. Attention is stressed to the interaction of the liquid film with some obstacle. S. G. Taylor [Proc. R. Soc. London Ser. A 253, 313 (1959)] found that the liquid film generated by impinging jets is very sensitive to properties of the wire which was used as an obstacle. The aim of this presentation is to propose a modification of the Taylor's model, which allows to simulate the film shape in cases, when the angle between jets is different from 180°. Numerical results obtained by discussed models give two different shapes of the liquid film similar as in Taylors experiments. These two shapes depend on the regime: either droplets are produced close to the obstacle or not. The difference between two regimes becomes larger if the angle between jets decreases. Existence of such two regimes can be very essential for some applications of impinging jets, if the generated liquid film can have a contact with obstacles.
Keywords:
impinging jets, liquid film, models, numerical solution, shape
(22 S., 2001)

28. I. Ginzburg, K. Steiner

Free surface lattice-Boltzmann method to model the filling of expanding cavities by Bingham Fluids

The filling process of viscoplastic metal alloys and plastics in expanding cavities is modelled using the lattice Boltzmann method in two and three dimensions. These models combine the regularized Bingham model for viscoplastic with a free-interface algorithm. The latter is based on a modified immiscible lattice Boltzmann model in which one species is the fluid and the other one is considered as vacuum. The boundary conditions at the curved liquid-vacuum interface are met without any geometrical front reconstruction from a first-order Chapman-Enskog expansion. The numerical results obtained with these models are found in good agreement with available theoretical and numerical analysis.
Keywords:
Generalized LBE, free-surface phenomena, interface boundary conditions, filling processes, Bingham viscoplastic model, regularized models
(22 S., 2001)

29. H. Neunzert

»Denn nichts ist für den Menschen als Menschen etwas wert, was er nicht mit Leidenschaft tun kann«

Vortrag anlässlich der Verleihung des Akademiepreises des Landes Rheinland-Pfalz am 21.11.2001

Was macht einen guten Hochschullehrer aus? Auf diese Frage gibt es sicher viele verschiedene, fachbezogene Antworten, aber auch ein paar allgemeine Gesichtspunkte: es bedarf der »Leidenschaft« für die Forschung (Max Weber), aus der dann auch die Begeisterung für die Lehre erwächst. Forschung und Lehre gehören zusammen, um die Wissenschaft als lebendiges Tun vermitteln zu können. Der Vortrag gibt Beispiele dafür, wie in angewandter Mathematik Forschungsaufgaben aus praktischen Alltagsproblemstellungen erwachsen, die in die Lehre auf verschiedenen Stufen (Gymnasium bis Graduiertenkolleg) einfließen; er leitet damit auch zu einem aktuellen Forschungsgebiet, der Mehrskalenanalyse mit ihren vielfältigen Anwendungen in Bildverarbeitung, Materialentwicklung und Strömungsmechanik über, was aber nur kurz gestreift wird. Mathematik erscheint hier als eine moderne Schlüsseltechnologie, die aber auch enge Beziehungen zu den Geistes- und Sozialwissenschaften hat.
Keywords:
Lehre, Forschung, angewandte Mathematik, Mehrskalenanalyse, Strömungsmechanik
(18 S., 2001)

30. J. Kuhnert, S. Tiwari

Finite pointset method based on the projection method for simulations of the incompressible Navier-Stokes equations

A Lagrangian particle scheme is applied to the projection method for the incompressible Navier-Stokes equations. The approximation of spatial derivatives is obtained by the weighted least squares method. The pressure Poisson equation is solved by a local iterative procedure with the help of the least squares method. Numerical tests are performed for two dimensional cases. The Couette flow, Poiseuelle flow, decaying shear flow and the driven cavity flow are presented. The numerical solutions are obtained for stationary as well as instationary cases and are compared with the analytical solutions for channel flows. Finally, the driven cavity in a unit square is considered and the stationary solution obtained from this scheme is compared with that from the finite element method.
Keywords:
Incompressible Navier-Stokes equations, Meshfree method, Projection method, Particle scheme, Least squares approximation
AMS subject classification:
76D05, 76M28
(25 S., 2001)

31. R. Korn, M. Krekel

Optimal Portfolios with Fixed Consumption or Income Streams

We consider some portfolio optimisation problems where either the investor has a desire for an a priori specified consumption stream or/and follows a deterministic pay in scheme while also trying to maximize expected utility from final wealth. We derive explicit closed form solutions for continuous and discrete monetary streams. The mathematical method used is classical stochastic control theory.
Keywords:
Portfolio optimisation, stochastic control, HJB equation, discretisation of control problems.
(23 S., 2002)

32. M. Krekel

Optimal portfolios with a loan dependent credit spread

If an investor borrows money he generally has to pay higher interest rates than he would have received, if he had put his funds on a savings account. The classical model of continuous time portfolio optimisation ignores this effect. Since there is obviously a connection between the default probability and the total percentage of wealth, which the investor is in debt, we study portfolio optimisation with a control dependent interest rate. Assuming a logarithmic and a power utility function, respectively, we prove explicit formulae of the optimal control.
Keywords:
Portfolio optimisation, stochastic control, HJB equation, credit spread, log utility, power utility, non-linear wealth dynamics
(25 S., 2002)